COMPARISON OF MICROSTRUCTURES AND MECHANICAL PROPERTIES FOR SOLID COBALT-BASE ALLOY COMPONENTS AND BIOMEDICAL IMPLANT PROTOTYPES FABRICATED BY ELECTRON BEAM MELTING

S. M. Gaytan[1,2], L. E. Murr[1,2], E. Martinez[1,2], J. L. Martinez[1,2], B. I. Machado[1], D. A. Ramirez[1],
F. Medina[2], S. Collins[3] and R. B. Wicker[2]

[1] Department of Metallurgical and Materials Engineering
The University of Texas at El Paso, El Paso, TX 79968 USA
[2] W. M. Keck Center for 3D Innovation
The University of Texas at El Paso, El Paso, TX 79968 USA
[3] Additive Manufacturing Processes, 4995 Paseo Montelena, Camarillo, CA 93012 USA

ABSTRACT

The microstructures and mechanical behavior of simple, as-fabricated, solid geometries (with a density of 8.4 g/cm^3), as-fabricated and fabricated and annealed femoral (knee) prototypes all produced by additive manufacturing (AM) using electron beam melting (EBM) of Co-26Cr-6Mo-0.2C powder are examined and compared in this study. Microstructures and microstructural issues are examined by optical metallography, SEM, TEM, EDS, and XRD while mechanical properties included selective specimen tensile testing and Vickers microindentation (HV) and Rockwell C-scale (HRC) hardness measurements. Orthogonal (X-Y) melt scanning of the electron beam during AM produced unique, orthogonal and related $Cr_{23}C_6$ carbide (precipitate) cellular arrays with dimensions of ~2μm in the build plane perpendicular to the build direction, while connected carbide columns were formed in the vertical plane, parallel to the build direction.

INTRODUCTION

The evolution of manufacturing technologies implies the need of characterizing different materials available in order to obtain the best properties intended for the specific applications. Rapid manufacturing by electron beam melting is becoming an ideal technology to create complex shapes through computer-controlled self-assembly by sintering or melting of powder layers [1]. Since traditional manufacturing consists of creating a final shape by the use of substractive or formative processes, rapid prototyping consists of forming a model, one layer at a time, from bottom to top [2]. By combining 3D implant models and rapid prototyping technologies gives us the capability of fabricating custom anatomical implants [3].

Nowadays some manufacturing enterprises have started to use rapid prototyping methods (or additive manufacturing, AM) for complex pattern making and component prototyping to shorten the time for pattern, molds and prototype development [4].

The powder material utilized for this project is Co-26Cr-6Mo-0.2C since it is an alloy that can withstand high temperatures, and has a high wear resistance, it can be used in gas turbines; valve seats, nuclear power plants, automobile engines, aerospace fuel nozzles and engine vanes and components, as well as in a variety of orthopaedic and dental implants [5-8].

METHODS AND PROCEDURES

Electron beam melting was utilized to fabricate CoCrMo specimens to be analyzed by optical microscopy and transmission electron microscopy, in addition, hardness and tensile testing was performed. A schematic of the EBM system is shown in figure 1a, the EBM system is computer driven and works in vacuum. Number 1 shows the location of the electron gun operating at 60kV, the beam depicted in number 2 is focused and bent by electromagnetic scan coils. Number 3 shows the location of the powder to be used for the process while number 4 shows the building table that moves down ~100μm to provide a new layer of powder. The basic operation procedure of the EBM consists of preheating and then melting the desired areas in each layer, at an approximate temperature of 830°C, as directed by the STL file created. Once the components were fabricated they were optically analyzed in the vertical and the horizontal planes which can also be more specifically described as parallel and perpendicular to the building direction respectively. In addition to analyzing as-fabricated components an annealed and rough polished component in the shape of a femoral-knee implant was also analyzed. The annealing heat treatment consisted of initial hot isostatic pressing (HIP) at ~1200°C for 4h in Ar at 10^3 bar, followed by quench from a homogenizing treatment at 1220°C for 4h in Ar, at 75°C/min. The homogenizing temperature was ~0.8 T_M (~1430°C), and everything was performed following ASTM F75 CoCr Alloy standard [9].

More than one etching solution had to be used to complete this study, to begin with a solution consisting of 6:1 HCL:H_2O_2 (3%) for 16 h for the as-fabricated components while the annealed component used a solution consisting of 6:1 HCL:H_2O_2 for an average time of 5 minutes. The solution utilized for the TEM specimens consisted of 15% $HClO_4$ and 85% acetic acid deposited in a jet polisher system (Tenupol-5) at a temperature range of 25-40°C and 20V.

XRD spectra were obtained from a Brucker AXS-D8 system using a Cu target. A Vickers hardness (HV) indenter (25-100 gf (0.25-1N) load at ~10s load time in a Shimadzu HMV-2000 system and a Rockwell C-scale hardness (HRC) tester (1.5 kN load) were used for this project while tensile testing was performed in an Instron system at ambient temperatures (~ 20°C) at a strain rate of $3x10^{-3}s^{-1}$.

RESULTS AND DISCUSSION

Figure 1b shows CoCrMo powder used for this project, having a nominal powder size diameter of 40μm. A higher magnification SEM micrograph of the CoCrMo powder is shown in figure 2. Microstructural characterization was performed in the EBM fabricated components obtaining a unique and complex array of carbides as the one illustrated in figure 3. Figure 3 was obtained from the vertical plane of a cylindrical component (the arrow shows the building direction) with dimensions consisting of a diameter of 1.5 cm and ~11 cm in length. The vertical plane of any component stands for the parallel plane related to the building direction, while the horizontal plane stands for the plane perpendicular to the same. It is also important to mention that cylinders of these dimensions were utilized to machine tensile test specimens for this project.
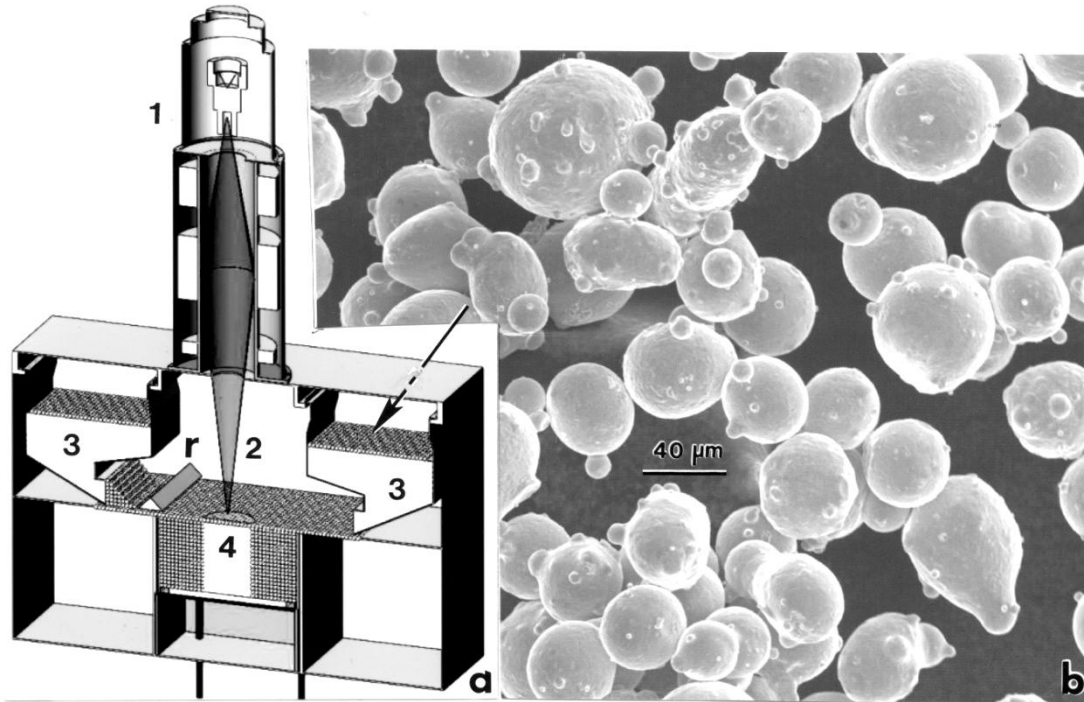
Figure 1. (a) EBM system schematic. (b) SEM image of CoCrMo powder particles

XRD was performed on the CoCrMo powder before being utilized by the EBM system, on the horizontal plane of as-fabricated cylindrical specimens and also on an annealed and rough polished section cut from a femoral knee implant component shape as illustrated in figure 4. It can be observed how the cylindrical component shows a variety of crystallographic and compositional phase mixtures, mostly hcp with a Co or CoCr fcc matrix. The carbide found is $Cr_{23}C_6$ which is an fcc with a lattice parameter of 10.66A°. It can be appreciated how the carbide peak is absent in the annealed and polished knee component, which is also observed from the metallographic images obtained for this specimen when comparing figure 5 to figure 6. In figure 5 the regular carbide arrays representing precipitation are created by the cross-scanning of the electron beam during preheating and in suceessive layer building, with dimensions of ~2μm are observed in the horizontal plane while similarly spaced columns of carbides are shown extending along the build direction. Other regular and irregular columnar carbide features are observed in the vertical plane view in figure 5a with dimensions similar to those shown in the horizontal plane. Figure 6 shows the microstructure obtained from a small section of the annealed and polished component revealing an equiaxed fcc grain structure and annealing twins.
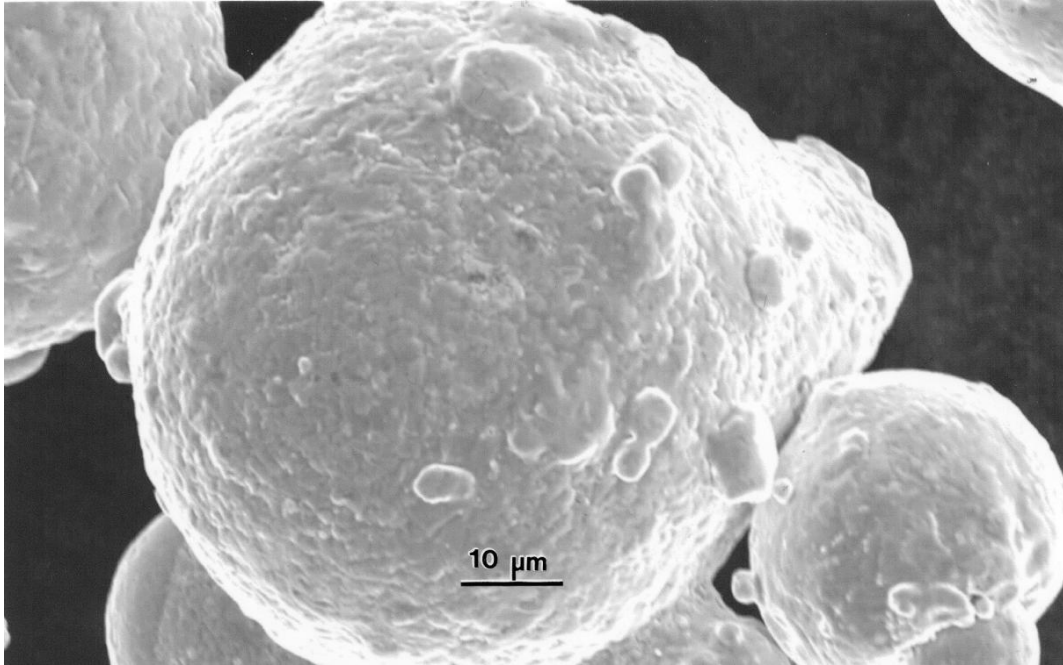
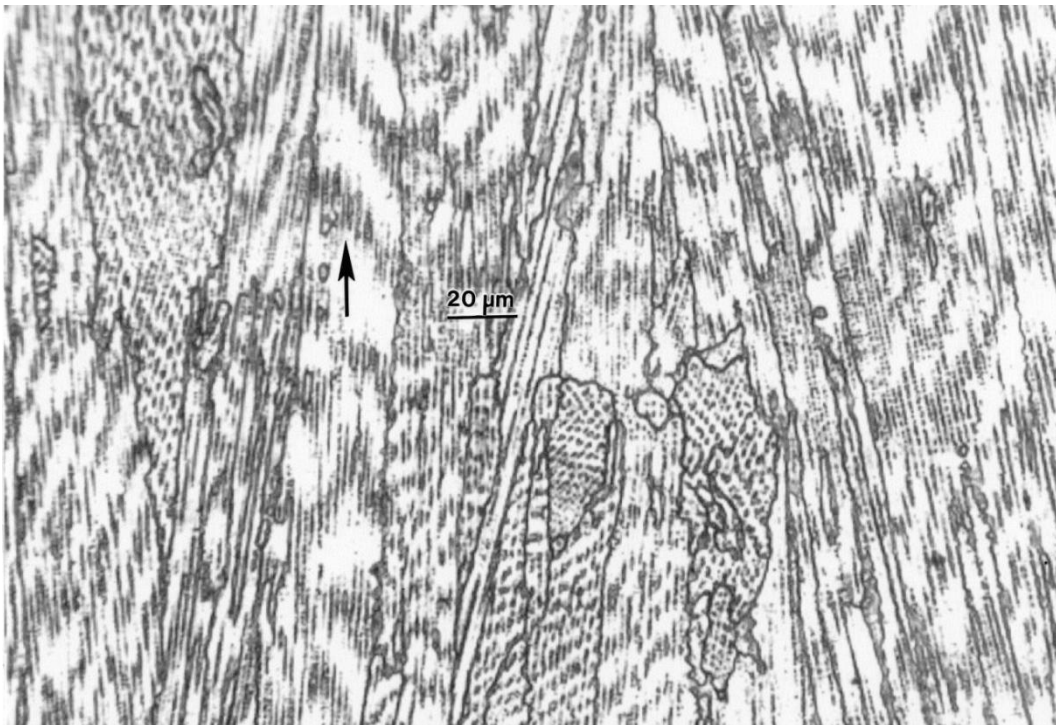**Figure 2. High magnification SEM image of CoCrMo powder**

Figure 3. Vertical plane of a cylindrical component fabricated by EBM showing a unique and complex array of carbides
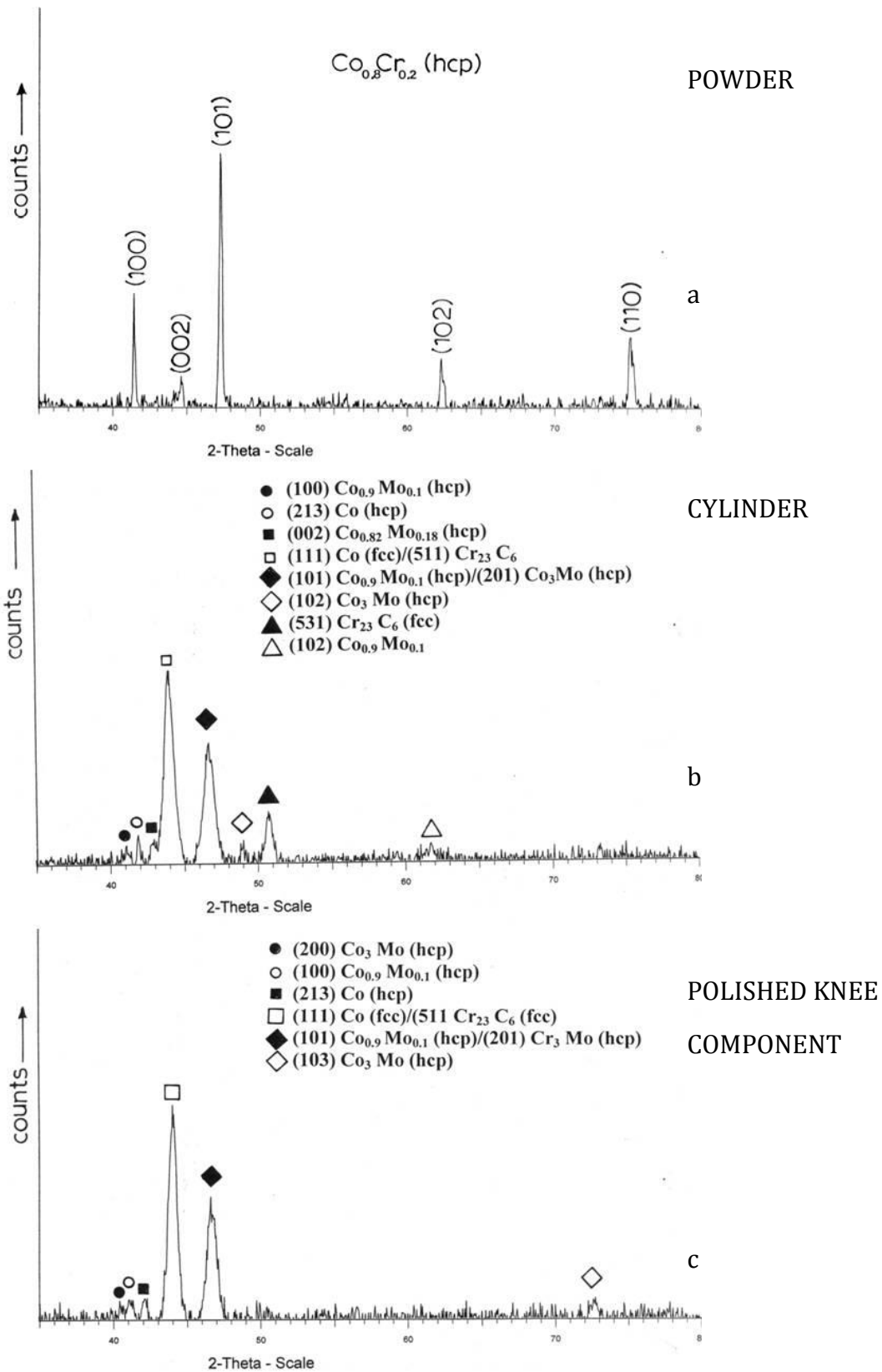
Figure 4. XRD spectrum for precursor powder, horizontal plane of cylindrycal component and annealed and polished femoral (knee) component
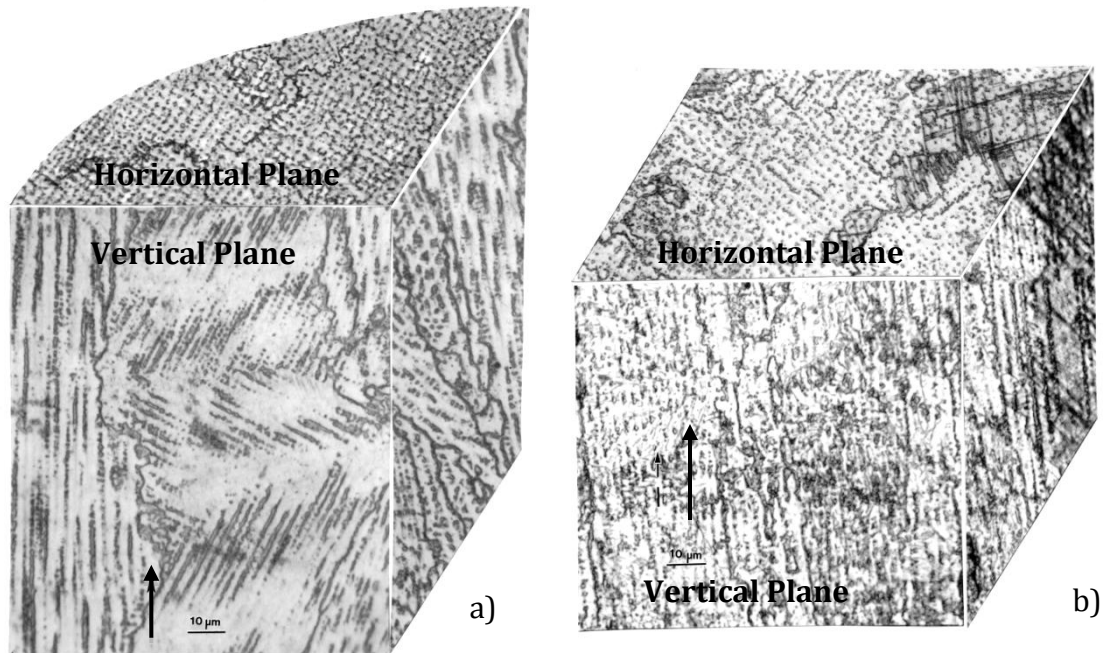
Figure 5. 3D metallographic representation of cylindrical component (a) and block component (b). Arrow indicates build direction
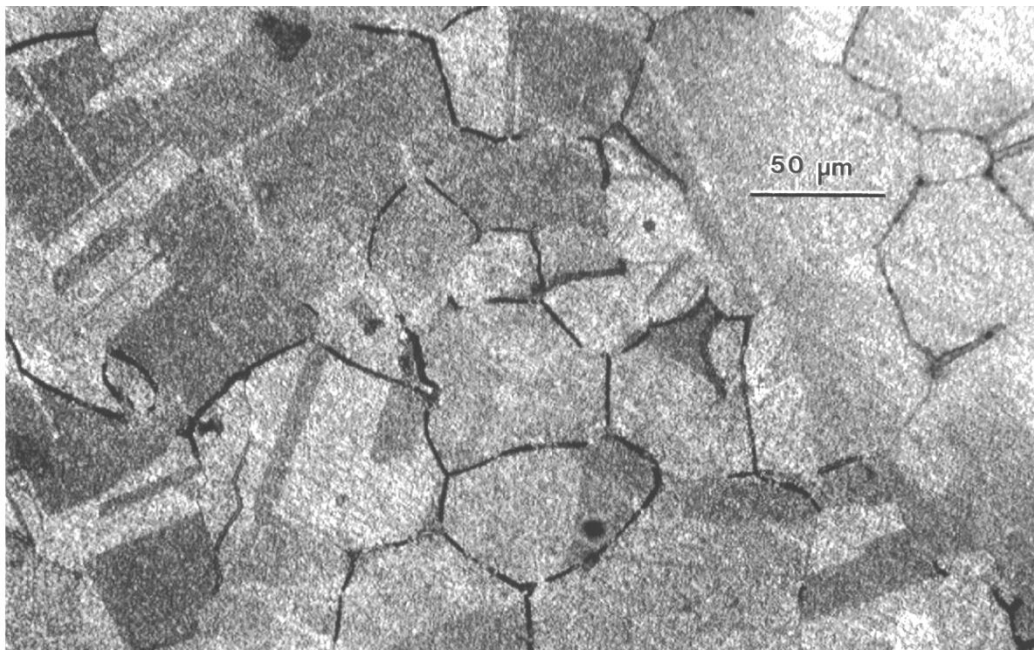

Figure 6. Optical metallographic view for the annealed and polished femoral knee component showing an equiaxed, fcc grain structure containing annealing twins

Figure 7 is a TEM image obtained from a cylindrical component's horizontal plane. It can be observed how $Cr_{23}C_6$ precipitates are present along with stacking faults and dislocations. From the selected area electron diffraction (SAED) pattern it can be observed the presence of the fcc Co matrix spots combined with the precipitate related spots belonging to the fcc (100) $Cr_{23}C_6$ pointed by the small arrow close to the beam stopper. Figure 8 shows a low and high magnification TEM image representing the vertical and horizontal planes of as-fabricated EBM components. A columnar array of $Cr_{23}C_6$ precipitates shows to be spaced approximately 100 to 200nm. It can also be appreciated from figure 8b that dislocation arrangements are intermingled with carbide precipitates as well as contrast fringes indicating linear stacking-fault features, present in both horizontal and vertical plane views. Figure 9 is a TEM image from an annealed and polished femoral knee component showing a greater stacking fault density in contrast to figures 7 and 8. It can also be observed from the SAED pattern that there is no evidence of $Cr_{23}C_6$ carbide precipitates and the (100) fcc SAED pattern exhibits a calculated lattice parameter of 3.55 Å, consistent with fcc Co.
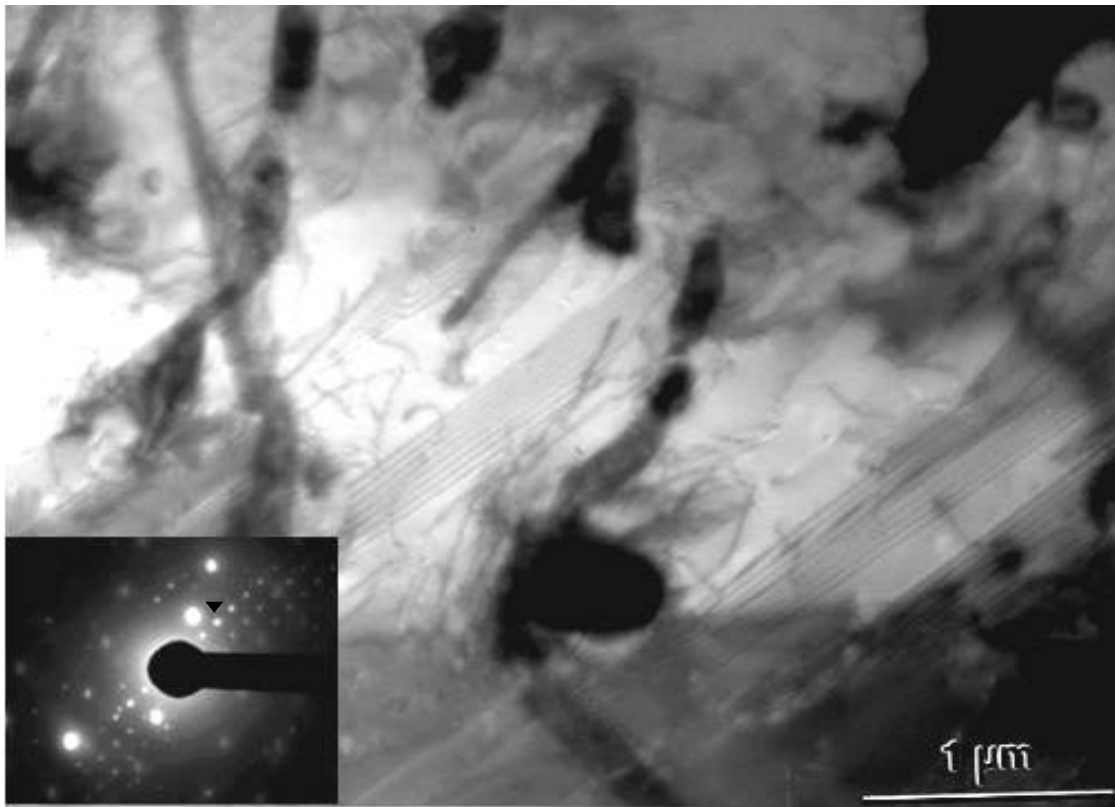

Figure 7. TEM bright-field image of the horizontal plane for a cylindrical component showing Cr₂₃C₆ precipitates, dislocations and stacking faults. The SAED pattern insert shows fcc Co (matrix) diffraction spots and (100) fcc Cr₂₃C₆ diffraction spots (arrow)
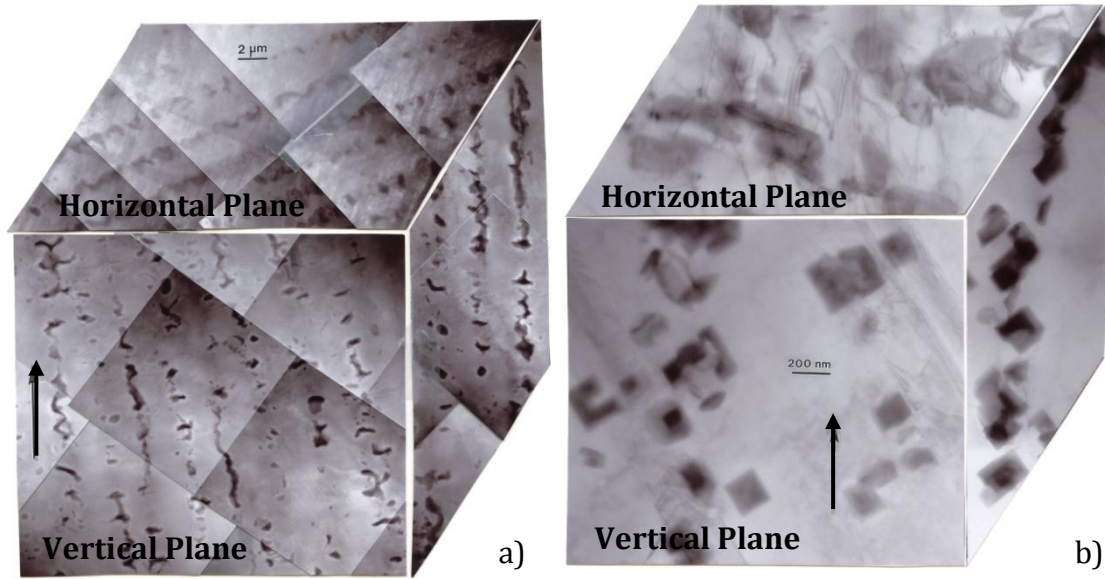
Figure 8. Shows a 3D representation of TEM images showing columnar arrays of $Cr_{23}C_6$ precipitates (a) and at a higher magnification (b)
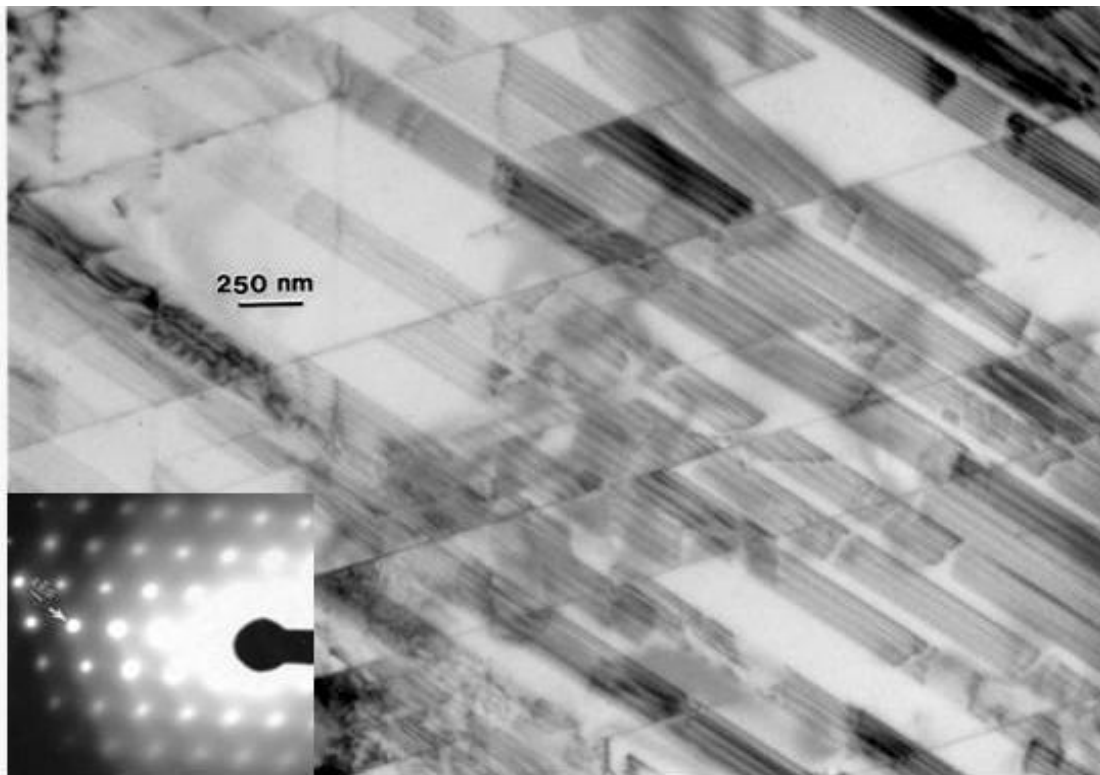

Figure 9. TEM bright-field image showing high density of intrinsic stacking faults on (111) planes coincident with the [2$\bar{2}$0] crystal direction shown in the SAED (110) pattern insert. Representative (110) grain in an annealed and polished femoral (knee) component

Table 1. Mechanical properties for EBM fabricated CoCrMo components

COMPONENT	HARDNESS		TENSILE[✣]		
	HV[*] (GPa)	HRC[**]	YIELD STRESS (GPa) [✣*✣]	UTS (GPa)	Elongation (%)
Precursor Powder	6.3	--	--	--	--
Solid Block	4.4*[✣]	44/46[✣✣]	--	--	--
Solid Cylinder	4.6*[✣]	47/48[✣✣]	0.51	1.45	3.6
As-Fabricated Knee (femoral)	5.9	46	--	--	--
Annealed/Polished Knee (femoral)	4.7	40	--	--	--

*Vickers microindentation hardness (VHN or HV) : 1 VHN= 0.01 GPa.

**Rockwell C-scale hardness

*[v]Horizontal plane (see figure 5)

[v]Average for 2 tests

[vv]Horizontal plane hardness/Vertical plane hardness (see figure 5)

[v*v]0.2% engineering offset yield stress.

Table 1 shows the tensile test results of specimens prepared from as-fabricated cylindrical components as well as the HV hardness test results for precursor powder, as-fabricated and annealed components as well as HRC hardness in the vertical and horizontal plane of cylindrical and block shape components and the annealed femoral-knee component. The yield stress is consistent with wrought and cast products, while UTS is considerably higher than as-cast or wrought ASTM F75 Co-Cr-Mo alloy, where nominally the yield stress and UTS are 0.5 GPa and 0.9 GPa respectively. An average elongation of 3.6% was obtained from two tensile samples where one value was 1.9% and the other 5.3%, when compared to as-cast ASTM F75 CoCrMo the elongation is <1% while wrought CoCrMo has an elongation of ~5%.

CONCLUSIONS

The EBM fabrication of components and prototypes from Co-26Cr-6Mo-0.2C powder ($Co_{0.8}Cr_{0.2}$ hcp crystal structure) creates Co-26Cr-6Mo-0.2C monoliths having fcc CoCr matrix with CrMo phase components and a unique, electron beam scan-produced $Cr_{23}C_6$ fcc orthogonal carbide array when viewed perpendicular to the build direction, and carbide columns connected to these arrays when viewed in a plane parallel to the build direction. In the same manner, after annealing, an equiaxed, fcc CoCr grain structure containing {111} coincident annealing twin forms with $Cr_{23}C_6$ carbides mainly in high energy grain boundary positions. TEM images demonstrate a high density of intrinsic stacking faults on {111} planes, and no matrix carbides. Tensile testing of as-fabricated EBM cylindrical components showed improved properties compared to wrought or cast Co-26Cr-0.6Mo alloys such as ASTM F75.

REFERENCES

[1] Murr, L. E., et al. 2009. Microstructure and mechanical behavior of Ti-6Al-4V produced by rapid-layer manufacturing, for biomedical applications. Journal of the Mechanical Behavior of Biomedical Materials, Vol 2, (1). 20-32.

[2] Kamrani, A. K., Nasr E. A., 2006. Rapid Prototyping. Theory and Practice. Springer Science+ Business Media, Inc.

[3] Vail, N. K., et al. 1999. Materials for biomedical applications. Materials and Design 20. 123-132.

[4] Yan, X. and Gu, P. 1996. Survey: A review of rapid prototyping technologies and systems. Computer-Aided Design. Vol 28, No. 4. 307-318.

[5] Antony, K. C. 1983. Wear-resistant cobalt base alloys. J. metals 35 (1983) 52-60.

[6] Alamert, S., and Bhadeshia, H.K.D.H. 1989. Comparison of the microstructure and abrasive wear properties of Stellite hardfacing alloys deposited by arc welding and laser cladding. Metals Technol. 20. 1037-1054.

[7] Shin, J., et al. 2003. Effect of molybdenum on the microstructure and wear resistance of cobalt-base Stellite alloys, Surf. Coat. Technol. 166. 117-126.

[8] ARCAM. ASTM F75 CoCr Alloy. Arcam EBM System. May 2010. <http://www.arcam.com/CommonResources/Files/www.arcam.com/Documents/EBM%20Materials/Arcam-ASTM-F75-Cobalt-Chrome.pdf>

[9] Gaytan, S. M., Murr, L. E., Martinez, E., Martinez, J. L., Machado, B. I., Ramirez, D. A., Medina, F., Collins, S., Wicker, R. B., (2010) to be published.